THE JOURNAL OF PHYSICAL CHEMISTRY A
Article
Cite This: J. Phys. Chem. A XXXX, XXX, XXX−XXX
pubs.acs.org/JPCA

Excited States of Methylene, Polyenes, and Ozone from Heat-Bath Configuration Interaction

Alan D. Chien,[†] Adam A. Holmes,[‡,¶] Matthew Otten,[¶] C. J. Umrigar,[*,¶] Sandeep Sharma,[*,‡] and Paul M. Zimmerman[*,†]

[†]Department of Chemistry, University of Michigan, Ann Arbor, Michigan 48109, United States
[‡]Department of Chemistry and Biochemistry, University of Colorado Boulder, Boulder, Colorado 80302, United States
[¶]Laboratory of Atomic and Solid State Physics, Cornell University, Ithaca, New York 14853, United States

ABSTRACT: The electronically excited states of methylene (CH_2), ethylene (C_2H_4), butadiene (C_4H_6), hexatriene (C_6H_8), and ozone (O_3) have long proven challenging due to their complex mixtures of static and dynamic correlations. The semistochastic heat-bath configuration interaction (SHCI) algorithm, which efficiently and systematically approaches the full configuration interaction (FCI) limit, is used to provide close approximations to the FCI energies in these systems. This article presents the largest FCI-level calculation to date on hexatriene, using a polarized double-ζ basis (ANO-L-pVDZ), which gives rise to a Hilbert space containing more than 10^{38} determinants. These calculations give vertical excitation energies of 5.58 and 5.59 eV, respectively, for the 2^1A_g and 1^1B_u states, showing that they are nearly degenerate. The same excitation energies in butadiene/ANO-L-pVDZ were found to be 6.58 and 6.45 eV. In addition to these benchmarks, our calculations strongly support the presence of a previously hypothesized ring-minimum species of ozone that lies 1.3 eV higher than the open-ring-minimum energy structure and is separated from it by a barrier of 1.11 eV.

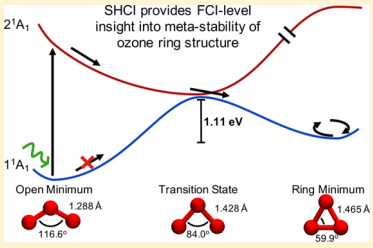

INTRODUCTION

The exponential increase in the Hamiltonian dimension with increasing system size means that exact Born−Oppenheimer electronic energies are not easily achievable for polyatomic molecular systems.[1−7] Recent years have seen impressive progress in methods that produce FCI-quality energies at greatly reduced cost, such as the density matrix renormalization group (DMRG),[8−12] FCI quantum Monte Carlo (FCIQMC),[13−16] and incremental FCI (iFCI).[17−19]

Another avenue for obtaining FCI-quality energies has also recently become available due to the revival of the selected configuration interaction plus perturbation theory (SCI+PT) algorithms. SCI+PT consists of two steps. In the first step, the most important determinants of the wave function of interest are identified iteratively, and the Hamiltonian in this subspace ($\mathcal{V}$) is diagonalized to obtain variational energies and wave functions. In the second step, the perturbative step of SCI+PT attempts to correct these energies and wave functions. The first such SCI+PT method was called Configuration Interaction by Perturbatively Selecting Iteratively (CIPSI), which established the basic steps of the SCI+PT algorithms.[20−25] Since then, many variations of CIPSI have been developed over the years,[26−50] all of which try to improve upon the CIPSI algorithm. However, a common drawback of all these variants is that, to construct the selected space $\mathcal{V}$ iteratively, the algorithm has to loop over all the determinants connected to any determinant in the previous iteration of $\mathcal{V}$. This becomes prohibitively expensive as the size of space $\mathcal{V}$ increases to several million determinants. Some of us have recently proposed the heat-bath CI (HCI)[51] algorithm that eliminates this expensive step by changing the selection criterion such that it enables an algorithm that loops over only those determinants that will be included in the selected space $\mathcal{V}$, a small fraction of all the possible connected determinants. This results in orders of magnitude speed up over other variants of SCI+PT for this step of the algorithm. HCI was further improved by semistochastic evaluation of the pertubative energy in semi-stochastic HCI (SHCI),[52] which eliminated the need to store a long list of perturbative determinants in memory. SHCI's potential has been demonstrated in previous works, where it was shown to efficiently treat CI spaces orders of magnitude larger than is possible with conventional CI algorithms.[52−55]

In this paper, highly accurate benchmarks for electronically excited states of the polyatomics in Figure 1 are computed using SHCI. Methylene is presented as the first test case, due to its small size yet challenging electronic structure.[56] Additionally,

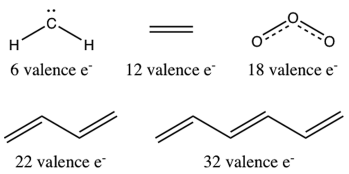

Figure 1. Molecules, methylene, ethylene, ozone, butadiene, and hexatriene, investigated with SHCI.

Received: February 13, 2018
Revised: February 22, 2018
Published: February 23, 2018

DOI: 10.1021/acs.jpca.8b01554
J. Phys. Chem. A XXXX, XXX, XXX−XXX

ozone is examined to answer a long-standing question regarding the existence of a theorized metastable ozone species.[57,58] Finally, SHCI is applied to the first few polyenes—ethylene, butadiene, and hexatriene—which have long been studied for their role as prototypical organic conducting polymers. The state ordering of the low-lying valence excited states, 2^1A_g and 1^1B_u, in butadiene and hexatriene have been especially challenging due to the significant numbers of highly correlated electrons and the near-degenerate nature of the valence states.[59−67] Herein, extrapolated SHCI state energies will provide high-accuracy $2^1A_g/1^1B_u$ state orderings in butadiene and hexatriene.

This article is organized as follows. In Methods, the excited-state SHCI algorithm is reviewed, and the path to convergence to the FCI limit is discussed. In Results and Discussion, results on the smaller methylene and ethylene systems are used to validate SHCI against current benchmark values and establish convergence with respect to FCI. These observations are then used to estimate FCI-quality energies for the larger ozone, butadiene, and hexatriene molecules. Conclusion provides closing remarks and an outlook on the SHCI method.

METHODS

Semistochastic Heat-Bath Configuration Interaction. As HCI and semistochastic perturbation theory have been described in detail,[51−53] only a brief overview will be given here. The HCI algorithm can be divided into variational and perturbative stages, each of which selects determinants through threshold values, ϵ_V and ϵ_{PT}, respectively. The current variational space of determinants is denoted by $\mathcal{V}$ and the space of all determinants connected by single or double excitations to $\mathcal{V}$, but not in $\mathcal{V}$, is denoted by $\mathcal{C}$.

The variational stage iteratively adds determinants to $\mathcal{V}$ by

1. Adding all determinants a connected to determinants in the current $\mathcal{V}$ that pass the importance criterion $\max_i |H_{ai}\ \max_n(|c_i^n|)|> \epsilon_V$, where c_i^n is the coefficient of determinant i in state n.
2. Constructing the Hamiltonian and solving for the roots of interest, in the basis of all determinants in the newly expanded $\mathcal{V}$.
3. Repeat 1−2 until convergence.

Convergence of the variational wave function for a given ϵ_V is signified by the addition of a small number of new determinants or small changes in the variational energy (E_{var}). The second-order Epstein−Nesbet perturbative energy correction (ΔE_2) is added to E_{var} to obtain the total HCI energy (E_{tot}). This correction is

$$\Delta E_2 = \sum_{a\in C} \frac{\left(\sum_{i\in\mathcal{V}}^{(\epsilon_{PT})} H_{ai}c_i\right)^2}{E_0 - H_{aa}} \quad (1)$$

where a runs over determinants in $\mathcal{C}$, and i runs over determinants in $\mathcal{V}$. Similar to the variational stage, the perturbation only considers the determinants connected to the final $\mathcal{V}$ space that have an importance measure greater than a parameter ϵ_{PT}, which is typically orders of magnitude smaller than ϵ_V. In both the variational and the perturbative stages, the fact that the number of *distinct* values of the double-excitation matrix elements scales only as N_{orb}^4 is used, to avoid ever looking at the unimportant determinants. Nevertheless, storing the full space of determinants used in the perturbative correction becomes a memory bottleneck for larger systems.

SHCI sidesteps this memory bottleneck using a semi-stochastic second-order perturbation correction.[52] In this procedure, the perturbative correction is split into deterministic and stochastic contributions. A larger ϵ_{PT}^d, automatically determined to correspond to a determinant space of manageable size depending on available computer memory, is first used to obtain a deterministic energy correction. The remaining correlation is then calculated stochastically by taking the difference of the second-order corrections evaluated with ϵ_{PT} and ϵ_{PT}^d. Samples are taken until the statistical error falls below a specified threshold.

Converging SHCI Energies to the FCI Limit. The target accuracy for total or relative energies are typically be chosen to be 1 or 1.6 mHa (1 kcal/mol, representing chemical accuracy), though for the smaller systems, it is easy to achieve much higher accuracy. In SHCI, the error in the variational energy can be straightforwardly estimated by the magnitude of the perturbative correction.

In methylene and ethylene, SHCI can provide such highly converged variational energies. In larger systems, however, converging the variational energy would require prohibitively large variational spaces. Instead, we fit the variational energy or the total energy, $E_{tot} = E_{var} + \Delta E_2$, to $E_{var} - E_{tot}$ using a quadratic function and use the fitted function to extrapolate to the limit where the perturbative correction is zero ($E_{var} - E_{tot} = 0$). The fit coefficients for variational and total energies are the same, except that the coefficients of the linear terms differ by one, so the two energies extrapolate to precisely the same value. There is not a well-defined method for estimating the extrapolation error, but a reasonable choice is one-fifth of the difference between the calculated energy with the smallest value of ϵ_V and the extrapolated energy. In many cases, the fitted function is very nearly linear (e.g., Figures 2, 4, and 5).

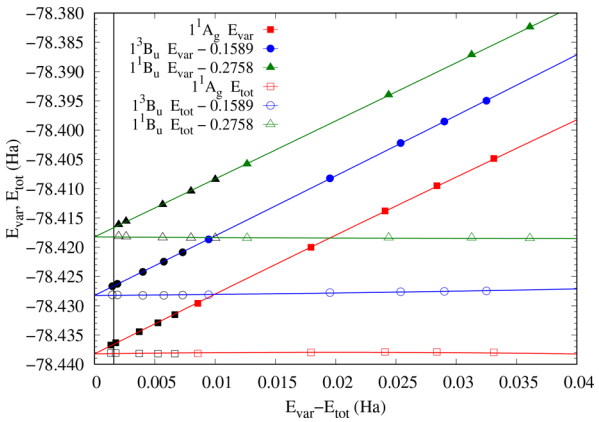

Figure 2. Fit of variational and total energies of ethylene using all data points. The black line is placed at 1.6 mHa. States are separated from one another by 0.01 Ha for clarity. The tightest SHCI calculation used $\epsilon_V = 7 \cdot 10^{-6}$ Ha. The extrapolated energies obtained using all data points are compared to those obtained by omitting the black points in Table 3.

Furthermore, even when the fitted functions are not close to linear, the functions for different states are often close to parallel, making the estimates of the energy differences particularly accurate.

Computational Details. SHCI is implemented in Fortran90, parallelized using MPI, and makes use of spatial symmetry and time-reversal symmetry when the number of up-

DOI: 10.1021/acs.jpca.8b01554
J. Phys. Chem. A XXXX, XXX, XXX−XXX

Table 1. Methylene/aug-cc-pVQZ Total (Ha) and Relative (eV) Energies

state	SHCI[a] aug-cc-pVQZ	CR-EOMCC (2,3)D[c] aug-cc-pVQZ	FCI[b] TZ2P		
1^3B_1	−39.08849(1)	−39.08817	−39.06674		
1^1A_1	−39.07404(1)	−39.07303	−39.04898		
1^1B_1	−39.03711(1)	−39.03450	−39.01006		
2^1A_1	−38.99603(1)	−38.99457	−38.96847		
gap	SHCI[a] aug-cc-pVQZ	CR-EOMCC (2,3)D[c] aug-cc-pVQZ	FCI[b] TZ2P	DMC[d]	exp
$1^1A_1-1^3B_1$	0.393	0.412	0.483	0.406	0.400[e]
$1^1B_1-1^3B_1$	1.398	1.460	1.542	1.416	1.411[f]
$2^1A_1-1^3B_1$	2.516	2.547	2.674	2.524	–

[a]Using $\epsilon_V = 10^{-5}$ Ha. [b]FCI/TZ2P results from ref 56. [c]This work. [d]Diffusion Monte Carlo results from ref 78. [e]References 56, 82. [f]References 56, 83.

Table 2. Ethylene/ANO-L-pVTZ Total (Ha) and Relative (eV) Energies

state	SHCI[a] ANO-L-pVTZ	CR-EOMCC(2,3)D[b] ANO-L-pVTZ	FCIQMC[c] ANO-L-pVTZ		
1^1A_g	−78.4381(1)	−78.43698	−78.4370(2)		
1^1B_{1u}	−78.1424(1)	−78.13375	−78.1407(3)		
1^3B_{1u}	−78.2693(1)	−78.26205	-		
gap	SHCI[a] ANO-L-pVTZ	CR-EOMCC(2,3)D[b] ANO-L-pVTZ	FCIQMC[c] ANO-L-pVTZ	iFCI[d] cc-pVTZ	exp
$1^1B_{1u}-1^1A_g$	8.05	8.25	8.06	-	7.66[e]
$1^3B_{1u}-1^1A_g$	4.59	4.76	-	4.64	4.3–4.6[f]

[a]E_{tot} with $\epsilon_V = 7 \cdot 10^{-6}$ Ha. [b]This work. [c]FCIQMC/ANO-L-pVTZ results from ref 71. [d]iFCI/cc-pVTZ results from ref 18. [e]Experimental band maximum from ref 87. [f]Experimental band maxima from references 88–90.

and down-spin electrons is equal.[52] The variational iterations are terminated when the number of new determinants added is less than 0.001% of the current variational space or when the change in variational energy is less than $1 \cdot 10^{-5}$ Ha. For all calculations, ϵ_{PT} is set to $1 \cdot 10^{-7}$ Ha, which provides converged perturbative corrections.[51,52] ϵ_V is made as small as possible on our hardware, obtaining either small ΔE_2 or enough data points to reliably extrapolate to $\Delta E_2 = 0$. The threshold for statistical error of the stochastic perturbative correction is generally set to $5 \cdot 10^{-5}$ Ha, although the larger hexatriene/ANO-L-pVDZ computations use $1 \cdot 10^{-4}$ Ha.

For the smaller systems (methylene and ethylene), achieving convergence is relatively easy, allowing the use of Hartree–Fock and HCI natural orbitals (obtained with $\epsilon_V = 3 \cdot 10^{-5}$ Ha), for methylene and ethylene respectively, to construct the molecular orbital integrals. For the larger systems (ozone, butadiene, hexatriene), the convergence was improved by using orbitals that minimize the HCI variational energy[54] for $\epsilon_V = 2 \cdot 10^{-4}$ Ha. Possibly, yet better convergence could be obtained by using orbitals that make the total energy stationary.[54]

Basis sets used are aug-cc-pVQZ[68,69] for methylene, ANO-L-pVTZ[70] for ethylene, ANO-L-pVDZ[70] for butadiene and hexatriene, and cc-pVTZ[68] for ozone. Geometries for methylene are FCI/TZVP quality taken from Sherrill et al.,[56] and ozone geometries are CASSCF(18,12)/cc-pVQZ quality, taken from Theis et al.[58] For the polyenes, all geometries are of MP2/cc-pVQZ quality, with ethylene and hexatriene geometries the same as in Zimmerman[18] and butadiene the same as in Alavi et al.[71] and Chan et al.[12] All calculations utilize the frozen-core approximation. For comparisons to coupled cluster theories, the same geometries and basis sets are used with the Q-Chem 4.0[72] CR-EOM-CC(2,3)D[73] implementation.[74]

RESULTS AND DISCUSSION

Methylene. Methylene is a prototypical test case for advanced electronic structure methods, being small enough to be amenable to canonical FCI benchmarks, yet still requiring accurate treatment of dynamic and static correlations for correct excitation energies.[56,75–81] The four lowest lying states of methylene vary in spin and spatial symmetry: 1^3B_1, 1^1A_1, 1^1B_1, and 2^1A_1. With only six valence electrons to correlate, SHCI can handily obtain FCI-quality energies even with the large aug-cc-pVQZ basis (Table 1), obtaining perturbative corrections less than 0.01 mHa with $\epsilon_V = 10^{-5}$ Ha.

Table 1 shows the most accurate SHCI adiabatic energy gaps calculated with $\epsilon_V = 10^{-5}$ Ha, which differ from experiment by about 0.01 eV. Comparing canonical FCI in the TZ2P basis with SHCI in the larger aug-cc-pVQZ basis shows differences of up to 0.158 eV,[56] demonstrating that large basis sets are necessary to fully describe correlation in methylene. This was first demonstrated using diffusion Monte Carlo (DMC) results,[78] which are much less sensitive to basis sets and agree with SHCI to within about 0.02 eV. CR-EOMCC(2,3)D relative energies are generally within 1.6 mHa (0.044 eV) of the benchmark SHCI values, indicating that high-level coupled cluster calculations are able to correlate six electrons sufficiently to obtain FCI-quality energy gaps.

Ethylene. Ethylene is another prototypical benchmark system for electronic excitations, including an especially challenging 1^1B_u state. Although the 1^1B_u state is qualitatively well described by a $\pi-\pi^*$ excitation, a quantitative description requires a thorough accounting of dynamic correlation between σ and π electrons.[84–86] Here, SHCI is applied to the low-lying valence states of ethylene: 1^1A_g, 1^1B_{1u}, and 1^3B_{1u}, in the ANO-L-pVTZ basis.

DOI: 10.1021/acs.jpca.8b01554
J. Phys. Chem. A XXXX, XXX, XXX–XXX

Fully correlating ethylene's 12 valence electrons is a considerably more difficult task than correlating methylene's 6. This is reflected in the fact that SHCI perturbative corrections start to fall below 1.6 mHa only at $\epsilon_V = 7 \cdot 10^{-6}$ Ha (Figure 2). These results suggest that polyatomics with up to 12 valence electrons and triple-ζ basis sets are amenable to treatment at the FCI level using just the variational component of SHCI. Table 2 compares SHCI total and relative energies with previous FCIQMC[71] and iFCI[18] results. SHCI total energies are only about 1 mHa lower than FCIQMC, and the $1^1B_{1u}-1^1A_g$ excitation energy is in even better agreement. The $1^3B_{1u}-1^1A_g$ energy obtained from iFCI is also in reasonably good agreement, though it is obtained using a different triple-ζ basis. On the other hand, Table 2 also indicates that coupled cluster methods must include more than triples excitations in order to obtain FCI-quality relative energies, as CR-EOMCC-(2,3)D results show errors considerably greater than 1.6 mHa (0.044 eV) with respect to the SHCI benchmark values. The SHCI relative energies support the notion that the vertical excitations cannot be quantitatively compared to the experimental band maxima in ethylene.[19,71]

Ethylene is the largest system tested for which the perturbative correction is less than 1.6 mHa. This requires using $\epsilon_V = 7 \cdot 10^{-6}$ Ha and 10^8 determinants in the variational space, which is near the limit of what can be reasonably stored on contemporary hardware.

As mentioned in Methods: Converging SHCI Energies to the FCI Limit, in larger systems we fit E_{tot} or E_{var} to $E_{var} - E_{tot}$ using a quadratic function and use the fitted function to extrapolate to the no perturbative correction limit, thereby obtaining accurate energies even when the variational energies are not converged.[53] The fits of E_{tot} and E_{var} are shown in Figure 2. The E_{tot} is nearly flat. To estimate the error of the extrapolation, we performed an additional fit omitting the black points in Figure 2. The extrapolated values obtained from the two fits are shown in Table 3.

Table 3. Comparison of Extrapolated Ethylene/ANO-L-pVTZ Energies Obtained Using All the Points Plotted in Figure 2 with Those Obtained from Omitting the Black Points

state	E_{extrap} (Ha) all points	E_{extrap} (Ha) omit black points
1^1A_g	−78.4382	−78.4385
1^1B_{1u}	−78.1424	−78.1430
1^3B_{1u}	−78.2693	−78.2697

Ozone. Ozone's potential energy surfaces have held great interest due to its role in atmospheric chemistry.[91] An interesting feature predicted by computational studies is the existence of a metastable ring geometry on the ground-state surface.[57] A lack of experimental evidence for such a species has fueled multiple studies of the pathway leading to the ring species over the years.[92−97] The most recent such study by Ruedenberg et al. utilizes multireference CI with up to quadruple excitations,[58] expending considerable effort on selecting and justifying an active space. To provide an accurate picture at critical points along the theorized pathway with even treatment of all valence electrons, SHCI is applied to ozone's $2^1A_1-1^1A_1$ gap with the cc-pVTZ basis at the three geometries of interest shown in Figure 3: the equilibrium geometry (termed the open-ring minimum (OM)), the hypothetical ring minimum (RM), and the transition state (TS) between these two.

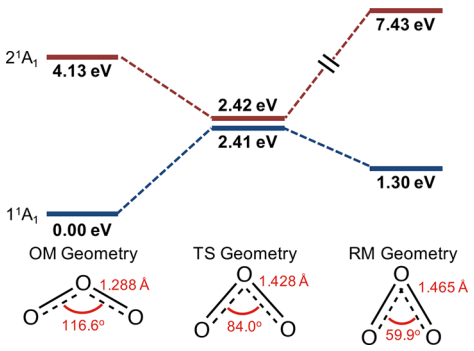

Figure 3. Ozone potential energy surface.

As anticipated, sub-mHa perturbative corrections cannot be readily obtained for ozone in the cc-pVTZ basis. ΔE_2 for the best available SHCI calculations, at $\epsilon_V = 4 \cdot 10^{-5}$ Ha, range from 15 to 28 mHa for the various geometries and states under consideration. The accuracy of ozone's extrapolated $2^1A_1-1^1A_1$ gaps can easily be corroborated for the OM and TS geometries, as the gaps over a broad range of ϵ_V's (Table 4) vary by less than 1 mHa, so the extrapolated values should be even more accurate. The RM geometry's gap is not as easily corroborated, as these vary over a 2.1 mHa range at reasonably tight ϵ_V's. Therefore, a conservative view would be to take the extrapolated gap as slightly less than chemically accurate.

Table 4. Evolution of Ozone $2^1A_1-1^1A_1$ Gaps (Ha)[a]

ϵ_V	OM	TS	RM
$2 \cdot 10^{-4}$	0.1520	0.0009	0.2897
$1 \cdot 10^{-4}$	0.1522	0.0008	0.2314
$5 \cdot 10^{-5}$	0.1521	0.0005	0.2298
$4 \cdot 10^{-5}$	0.1521	0.0006	0.2293
extrapolated	0.1519	0.0003	0.2254

[a]The RM energy at $\epsilon_V = 2 \cdot 10^{-4}$ is omitted from the fit.

In Table 5, the SHCI energy gaps are compared to Ruedenberg et al.'s MRCI results.[58] SHCI results mostly resemble the MRCI estimates, except for the RM geometry, where the gaps differ by more than 1 eV. The SHCI results, however, are sufficiently converged to allow valuable insights to be made into the metastable nature of the RM species. Along the 1^1A_1 potential surface, the RM and TS geometries lie 1.30 and 2.41 eV, respectively, above the OM geometry. These values suggest that electronic excitations in ozone are likely required to reach RM but that the RM species should be relatively stable with a 1.11 eV barrier hindering return to the OM geometry. Thus, SHCI indicates that a RM species may well exist, and that experimental investigations should be able

Table 5. Ozone $2^1A_1-1^1A_1$ Gaps (eV)

geometry	extrapolated SHCI	MRCI (SDTQ)[a]
OM	4.13	3.54−4.63
TS	0.01	0.05−0.16
RM	6.13	7.35−8.44

[a]Reference 58

DOI: 10.1021/acs.jpca.8b01554
J. Phys. Chem. A XXXX, XXX, XXX−XXX

to observe it if a plausible isomerization pathway can be accessed.

Shorter Polyenes: Butadiene and Hexatriene. Butadiene and hexatriene are part of the polyene series, long studied for their role as prototypical organic conducting polymers. In particular, the spacing of the low-lying valence excited states has proven especially challenging for electronic structure methods.[59−67] Butadiene and hexatriene are of special interest because their 1^1B_{1u} and 2^1A_g states are nearly degenerate, resulting in conflicting reports of state ordering at lower levels of theory. In the ANO-L-pVDZ basis, butadiene and hexatriene's FCI spaces of 10^{26} and 10^{38} determinants, respectively, are too large for the routine application of FCI-level methods, although limited FCIQMC[71] and DMRG[12] studies as well as SHCI ground-state calculations[53] have been performed on butadiene. Herein, SHCI is applied to the 1^1A_g, 1^1B_{1u}, 1^3B_{1u}, and 2^1A_g states to provide accurate benchmarks and state orderings.

Butadiene. Similar to ozone, extrapolation is used to obtain FCI energy estimates for butadiene in the ANO-L-pVDZ basis, as the tightest SHCI calculations at $\epsilon_V = 3 \cdot 10^{-5}$ Ha had perturbative corrections ranging from 12 to 29 mHa (Figure 4).

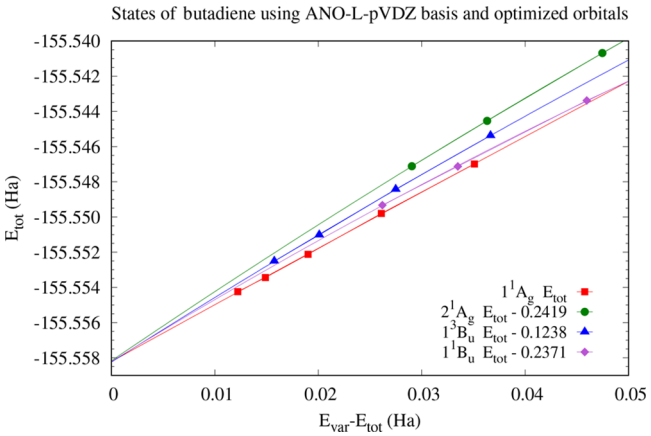

Figure 4. Extrapolation of butadiene SHCI energies. States shifted to extrapolate to the same energy. The tightest SHCI calculation used $\epsilon_V = 3 \cdot 10^{-5}$ Ha.

Besides using orbitals that minimize the SHCI variational energy, for molecules with more than a few atoms, a further improvement in the energy convergence can be obtained by localizing the orbitals. Butadiene has C_{2h} symmetry, but the localized orbitals transform as the irreducible representations of the C_s subgroup of C_{2h}. Both the A_g and the B_u irreducible representations of C_{2h} transform as the A″ representation of C_s. Hence, calculating the three singlet states 1^1A_g, 2^1A_g, and 1^1B_{1u} would require calculating three states simultaneously if localized orbitals are used, and further, we would not know if the 2^1A_g or the 1^1B_{1u} is lower in energy. Consequently, we calculated only the 1^1A_g and 1^3B_{1u} orbitals using localized orbitals and computed the 2^1A_g and 1^1B_{1u} states with extended orbitals.

Table 6 shows that using the same geometry as in prior FCIQMC,[71] DMRG,[12] and iFCI[19] calculations leads to a SHCI 1^1A_g energy that is 0.4 and 0.9 mHa below the extrapolated DMRG[98] and iFCI energies, respectively. Although FCIQMC has yielded very accurate energies for many systems, in the case of butadiene, all three methods (SHCI, iFCI, and DMRG) are in agreement that the FCIQMC energy for the 1^1A_g is 8−9 mHa too high. This may be either because of FCIQMC initiator bias or because of an underestimate of the FCIQMC statistical error because of the very long autocorrelation times encountered for large systems. A similar conclusion can be reached for the FCIQMC 1^1B_{1u} calculation, as the SHCI energy falls below it by a large amount, 12 mHa.

Table 6. Butadiene Total (Ha) and Relative Energies (eV)

state	extrapolated SHCI[a]	FCIQMC[b]	DMRG[c]	
1^1A_g	−155.5582(1)	−155.5491(4)	−155.5578	
1^3B_u	−155.4344(1)	-	-	
1^1B_u	−155.3211(1)	−155.3092(6)	-	
2^1A_g	−155.3163(1)	-	-	
gap	**extrapolated SHCI**	**FCIQMC[b]**	**iFCI[d]**	**exp**
$2^1A_g-1^1A_g$	6.58	-	-	-
$1^1B_u-1^1A_g$	6.45	6.53	-	5.92[e]
$1^3B_u-1^1A_g$	3.37	-	3.45	3.22[f]

[a]Extrapolation errors may range from a few tenths of a mHa for 1^1A_g to a couple of mHa for 2^1A_g. [b]FCIQMC/ANO-L-pVDZ results from ref 71. [c]DMRG/ANO-L-pVDZ extrapolated energy[98] using data from ref 12. [d]iFCI 6-31G* results from ref 18. [e]Experimental band maxima from references 102−104. [f]Experimental band maxima from ref 105.

Turning to relative energies, we see that SHCI is in close agreement with all prior FCI-level theoretical calculations. Both the $1^3B_u-1^1A_g$ and $1^1B_u-1^1A_g$ gaps are 0.08 eV away from the iFCI and FCIQMC values, respectively. Although the $2^1A_g-1^1A_g$ gap does not currently have FCI-level benchmarks, the agreement of SHCI's other relative energies with existing benchmarks supports the accuracy of the extrapolated SHCI value for this gap, which is 6.58 eV. This places the 2^1A_g state above 1^1B_u in butadiene by 0.13 eV. This small gap is consistent with recent theoretical[99] and experimental[100] investigations demonstrating ultrafast population transfer from 1^1B_u to 2^1A_g, which implies close proximity of the two states. As with ethylene, relative energies only qualitatively agree with experiment, supporting prior indications that experimental band maxima of butadiene do not correspond to the vertical excitation energy.[101]

Hexatriene. Hexatriene is at the current frontier of FCI-level computations, with a demanding FCI space of 10^{38} determinants in the ANO-L-pVDZ basis. Only one other algorithm, iFCI,[18] has approached FCI energies for such a large polyatomic—and then only for its singlet−triplet gap. Here we compute the energies of the lowest three singlet states and the lowest triplet state, using values of ϵ_V as small as $2 \cdot 10^{-5}$ Ha (Figure 5), which results in as many as $9 \cdot 10^7$ variational determinants.

The extrapolated hexatriene energies are reported in Table 7. With the same geometry, SHCI produces a 1^1A_g total energy 4 mHa below that of iFCI. This difference is within the extrapolation uncertainty of SHCI for this system. Prior investigations of hexatriene photodynamics[106−108] place 1^1B_u close in energy to 2^1A_g. At the vertical excitation geometry, SHCI places 2^1A_g below 1^1B_u with a small gap of only 0.01 eV. The triplet−singlet $1^3B_u-1^1A_g$ gaps computed by SHCI and iFCI (using the slightly smaller 6-31G* basis) differ by only 0.04 eV. As in the case of butadiene, the SHCI $1^1B_u-1^1A_g$ gap differs significantly from experiment,[109] indicating that experimental band maxima do not correspond to vertical excitation energies in hexatriene.

DOI: 10.1021/acs.jpca.8b01554
J. Phys. Chem. A XXXX, XXX, XXX−XXX

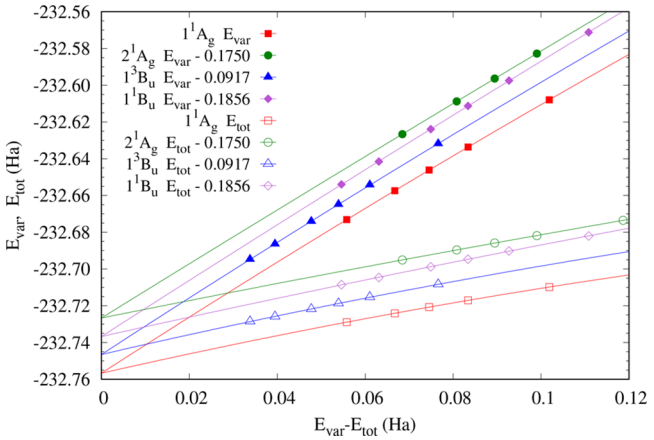

Figure 5. Extrapolation of hexatriene SHCI energies. States are separated from each other by 0.01 Ha for clarity. The tightest SHCI calculation used $\epsilon_V = 2 \cdot 10^{-5}$ Ha.

Table 7. Hexatriene Total (Ha) and Relative Energies (eV)

state	extrapolated SHCI		iFCI	
1^1A_g	−232.7567(1)		−232.7527[c]	
1^3B_u	−232.6548(1)		-	
1^1B_u	−232.5511(1)		-	
2^1A_g	−232.5517(1)		-	
gap	extrapolated SHCI	CC	iFCI	exp
2^1A_g−1^1A_g	5.58	5.72[a]	-	5.21[e]
1^1B_u−1^1A_g	5.59	5.30[a]	-	4.95[e], 5.13[e]
1^3B_u−1^1A_g	2.77	2.80[b]	2.81[d]	2.61[f]

[a]CR-EOMCC(2,3)D/TZVP from ref 67. [b]CCSD(T)/6-31G* from ref 18. [c]iFCI/ANO-L-pVDZ result from ref 19. [d]iFCI/6-31G* result from ref 18. [e]Raman scattering results from ref 110. [f]Electron impact band maximum from ref 111.

CONCLUSION

SHCI represents an important step forward for SCI methods, providing FCI-quality energies in the largest molecular systems to date. SHCI easily correlates systems of 12 electrons in a triple-ζ basis and can reach FCI-level energies in larger systems through extrapolation. In this paper, CI spaces of 10^7−10^8 determinants were used to effectively handle FCI spaces of 10^{26} and 10^{38} determinants.

This work has provided new benchmarks and insights for the valence states of some commonly investigated molecular systems. Specifically, high-quality SHCI energetics for ozone give strong evidence that the theorized RM structure has a significant barrier to relaxation and thus should be observable by experiment. Investigation of butadiene and hexatriene lead to the highest level $2^1A_g/1^1B_u$ state orderings in these systems to date, placing 2^1A_g above 1^1B_u in butadiene and minutely below 1^1B_u in hexatriene. In short, SHCI has shown itself to be an efficient means of obtaining FCI-level energetics, and we look forward to it providing physical insight into other chemically interesting systems with up to dozens of electrons.

AUTHOR INFORMATION

Corresponding Authors

*E-mail: cyrusumrigar@cornell.edu (C.J.U.)
*E-mail: sandeep.sharma@boulder.edu (S.S.)
*E-mail: paulzim@umich.edu (P.M.Z.)

ORCID

Alan D. Chien: 0000-0002-3103-0697
Sandeep Sharma: 0000-0002-6598-8887
Paul M. Zimmerman: 0000-0002-7444-1314

Notes

The authors declare no competing financial interest.

ACKNOWLEDGMENTS

A.D.C. and P.M.Z. would like to thank David Braun for computational support and the University of Michigan for financial support. S.S. acknowledges the startup package from the University of Colorado. A.A.H., M.O., and C.J.U. were supported in part by NSF grant ACI-1534965. Some of the computations were performed on the Bridges computer at the Pittsburgh Supercomputing Center, supported by NSF award number ACI-1445606.

REFERENCES

(1) Knowles, P.; Handy, N. A new determinant-based full configuration interaction method. *Chem. Phys. Lett.* **1984**, *111*, 315−321.
(2) Olsen, J.; Roos, B. O.; Jørgensen, P.; Jensen, H. J. A. Determinant based configuration interaction algorithms for complete and restricted configuration interaction spaces. *J. Chem. Phys.* **1988**, *89*, 2185−2192.
(3) Olsen, J.; Jørgensen, P.; Simons, J. Passing the one-billion limit in full configuration-interaction (FCI) calculations. *Chem. Phys. Lett.* **1990**, *169*, 463−472.
(4) Olsen, J.; Christiansen, O.; Koch, H.; Jørgensen, P. Surprising cases of divergent behavior in Møller-Plesset perturbation theory. *J. Chem. Phys.* **1996**, *105*, 5082−5090.
(5) Rossi, E.; Bendazzoli, G. L.; Evangelisti, S.; Maynau, D. A full-configuration benchmark for the N_2 molecule. *Chem. Phys. Lett.* **1999**, *310*, 530−536.
(6) Dutta, A.; Sherrill, C. D. Full configuration interaction potential energy curves for breaking bonds to hydrogen: An assessment of single-reference correlation methods. *J. Chem. Phys.* **2003**, *118*, 1610−1619.
(7) Gan, Z.; Grant, D. J.; Harrison, R. J.; Dixon, D. A. The lowest energy states of the group-IIIA-group-VA heteronuclear diatomics: BN, BP, AlN, and AlP from full configuration interaction calculations. *J. Chem. Phys.* **2006**, *125*, 124311.
(8) White, S. R. Density-matrix algorithms for quantum renormalization groups. *Phys. Rev. B: Condens. Matter Mater. Phys.* **1993**, *48*, 10345−10356.
(9) White, S. R.; Martin, R. L. Ab initio quantum chemistry using the density matrix renormalization group. *J. Chem. Phys.* **1999**, *110*, 4127−4130.
(10) Chan, G. K.-L.; Head-Gordon, M. Highly correlated calculations with a polynomial cost algorithm: a study of the density matrix renormalization group. *J. Chem. Phys.* **2002**, *116*, 4462−4476.
(11) Chan, G. K.-L.; Sharma, S. The density matrix renormalization group in quantum chemistry. *Annu. Rev. Phys. Chem.* **2011**, *62*, 465−481.
(12) Olivares-Amaya, R.; Hu, W.; Nakatani, N.; Sharma, S.; Yang, J.; Chan, G. K.-L. The ab-initio density matrix renormalization group in practice. *J. Chem. Phys.* **2015**, *142*, 034102.
(13) Booth, G. H.; Thom, A. J. W.; Alavi, A. Fermion Monte Carlo without fixed nodes: A game of life, death, and annihilation in Slater determinant space. *J. Chem. Phys.* **2009**, *131*, 054106.
(14) Cleland, D.; Booth, G. H.; Alavi, A. Communications: Survival of the fittest: Accelerating convergence in full configuration-interaction quantum Monte Carlo. *J. Chem. Phys.* **2010**, *132*, 041103.
(15) Petruzielo, F. R.; Holmes, A. A.; Changlani, H. J.; Nightingale, M. P.; Umrigar, C. J. Semistochastic projector Monte Carlo method. *Phys. Rev. Lett.* **2012**, *109*, 230201.

DOI: 10.1021/acs.jpca.8b01554
J. Phys. Chem. A XXXX, XXX, XXX−XXX

(16) Booth, G. H.; Gruneis, A.; Kresse, G.; Alavi, A. Towards an exact description of electronic wavefunctions in real solids. *Nature* **2013**, *493*, 365−370.
(17) Zimmerman, P. M. Incremental full configuration interaction. *J. Chem. Phys.* **2017**, *146*, 104102.
(18) Zimmerman, P. M. Singlet-triplet gaps through incremental full configuration interaction. *J. Phys. Chem. A* **2017**, *121*, 4712−4720.
(19) Zimmerman, P. M. Strong correlation in incremental full configuration interaction. *J. Chem. Phys.* **2017**, *146*, 224104.
(20) Huron, B.; Malrieu, J. P.; Rancurel, P. Iterative perturbation calculations of ground and excited state energies from multiconfigurational zeroth-order wavefunctions. *J. Chem. Phys.* **1973**, *58*, 5745−5759.
(21) Buenker, R. J.; Peyerimhoff, S. D. Energy extrapolation in CI calculations. *Theor. Chim. Acta* **1975**, *39*, 217−228.
(22) Buenker, R. J.; Peyerimhoff, S. D.; Butscher, W. Applicability of the multi-reference double-excitation CI (MRD-CI) method to the calculation of electronic wavefunctions and comparison with related techniques. *Mol. Phys.* **1978**, *35*, 771−791.
(23) Evangelisti, S.; Daudey, J. P.; Malrieu, J. P. Convergence of an improved CIPSI algorithm. *Chem. Phys.* **1983**, *75*, 91−102.
(24) Harrison, R. J. Approximating full configuration interaction with selected configuration interaction and perturbation theory. *J. Chem. Phys.* **1991**, *94*, 5021−5031.
(25) Ben Amor, N.; Bessac, F.; Hoyau, S.; Maynau, D. Direct selected multireference configuration interaction calculations for large systems using localized orbitals. *J. Chem. Phys.* **2011**, *135*, 014101.
(26) Buenker, R. J.; Peyerimhoff, S. D. Individualized configuration selection in CI calculations with subsequent energy extrapolation. *Theor. Chim. Acta* **1974**, *35*, 33−58.
(27) Langlet, J.; Gacoin, P. Excited states of phenyl carbonyl compounds. *Theor. Chim. Acta* **1976**, *42*, 293−301.
(28) Oliveros, E.; Riviere, M.; Teichteil, C.; Malrieu, J.-P. CI (CIPSI) calculations of the vertical ionization and excitation energies of the formamide molecule. *Chem. Phys. Lett.* **1978**, *57*, 220−223.
(29) Cimiraglia, R. Second order perturbation correction to CI energies by use of diagrammatic techniques: An improvement to the CIPSI algorithm. *J. Chem. Phys.* **1985**, *83*, 1746−1749.
(30) Cimiraglia, R.; Persico, M. Recent advances in multireference second order perturbation CI: The CIPSI method revisited. *J. Comput. Chem.* **1987**, *8*, 39−47.
(31) Knowles, P. J. Very large full configuration interaction calculations. *Chem. Phys. Lett.* **1989**, *155*, 513−517.
(32) Harrison, R. J. Approximating full configuration interaction with selected configuration interaction and perturbation theory. *J. Chem. Phys.* **1991**, *94*, 5021−5031.
(33) Povill, A.; Rubio, J.; Illas, F. Treating large intermediate spaces in the CIPSI method through a direct selected CI algorithm. *Theor. Chim. Acta* **1992**, *82*, 229−238.
(34) Steiner, M. M.; Wenzel, W.; Wilson, K. G.; Wilkins, J. W. The efficient treatment of higher excitations in CI calculations: A comparison of exact and approximate results. *Chem. Phys. Lett.* **1994**, *231*, 263−268.
(35) Garcia, V.; Castell, O.; Caballol, R.; Malrieu, J. An iterative difference-dedicated configuration interaction. Proposal and test studies. *Chem. Phys. Lett.* **1995**, *238*, 222−229.
(36) Wenzel, W.; Steiner, M.; Wilson, K. G. Multireference basis-set reduction. *Int. J. Quantum Chem.* **1996**, *60*, 1325−1330.
(37) Neese, F. A spectroscopy oriented configuration interaction procedure. *J. Chem. Phys.* **2003**, *119*, 9428−9443.
(38) Nakatsuji, H.; Ehara, M. Iterative CI general singles and doubles (ICIGSD) method for calculating the exact wave functions of the ground and excited states of molecules. *J. Chem. Phys.* **2005**, *122*, 194108.
(39) Abrams, M. L.; Sherrill, C. D. Important configurations in configuration interaction and coupled-cluster wave functions. *Chem. Phys. Lett.* **2005**, *412*, 121−124.
(40) Bytautas, L.; Ruedenberg, K. A priori identification of configurational deadwood. *Chem. Phys.* **2009**, *356*, 64−75.
(41) Roth, R. Importance truncation for large-scale configuration interaction approaches. *Phys. Rev. C: Nucl. Phys.* **2009**, *79*, 064324.
(42) Evangelista, F. A. A driven similarity renormalization group approach to quantum many-body problems. *J. Chem. Phys.* **2014**, *141*, 054109.
(43) Knowles, P. J. Compressive sampling in configuration interaction wavefunctions. *Mol. Phys.* **2015**, *113*, 1655−1660.
(44) Schriber, J. B.; Evangelista, F. A. Communication: An adaptive configuration interaction approach for strongly correlated electrons with tunable accuracy. *J. Chem. Phys.* **2016**, *144*, 161106.
(45) Liu, W.; Hoffmann, M. R. iCI: Iterative CI toward full CI. *J. Chem. Theory Comput.* **2016**, *12*, 1169−1178.
(46) Zhang, T.; Evangelista, F. A. A deterministic projector configuration interaction approach for the ground state of quantum many-body systems. *J. Chem. Theory Comput.* **2016**, *12*, 4326−4337.
(47) Scemama, A.; Applencourt, T.; Giner, E.; Caffarel, M. Quantum Monte Carlo with very large multideterminant wavefunctions. *J. Comput. Chem.* **2016**, *37*, 1866−1875.
(48) Garniron, Y.; Scemama, A.; Loos, P.-F.; Caffarel, M. Hybrid stochastic-deterministic calculation of the second-order perturbative contribution of multireference perturbation theory. *J. Chem. Phys.* **2017**, *147*, 034101.
(49) Giner, E.; Angeli, C.; Garniron, Y.; Scemama, A.; Malrieu, J.-P. A Jeziorski-Monkhorst fully uncontracted multi-reference perturbative treatment. I. Principles, second-order versions, and tests on ground state potential energy curves. *J. Chem. Phys.* **2017**, *146*, 224108.
(50) Schriber, J. B.; Evangelista, F. A. Adaptive configuration interaction for computing challenging electronic excited states with tunable accuracy. *J. Chem. Theory Comput.* **2017**, *13*, 5354−5366.
(51) Holmes, A. A.; Tubman, N. M.; Umrigar, C. J. Heat-bath configuration interaction: An efficient selected configuration interaction algorithm inspired by heat-bath sampling. *J. Chem. Theory Comput.* **2016**, *12*, 3674−3680.
(52) Sharma, S.; Holmes, A. A.; Jeanmairet, G.; Alavi, A.; Umrigar, C. J. Semistochastic heat-bath configuration interaction method: Selected configuration interaction with semistochastic perturbation theory. *J. Chem. Theory Comput.* **2017**, *13*, 1595−1604.
(53) Holmes, A. A.; Umrigar, C. J.; Sharma, S. Excited states using semistochastic heat-bath configuration interaction. *J. Chem. Phys.* **2017**, *147*, 164111.
(54) Smith, J. E. T.; Mussard, B.; Holmes, A. A.; Sharma, S. Cheap and near exact CASSCF with large active spaces. *J. Chem. Theory Comput.* **2017**, *13*, 5468−5478.
(55) Mussard, B.; Sharma, S. One-step treatment of spin-orbit coupling and electron correlation in large active spaces. *J. Chem. Theory Comput.* **2018**, *14*, 154−165.
(56) Sherrill, C. D.; Leininger, M. L.; Van Huis, T. J.; Schaefer, H. F. Structures and vibrational frequencies in the full configuration interaction limit: Predictions for four electronic states of methylene using a triple-zeta plus double polarization (TZ2P) basis. *J. Chem. Phys.* **1998**, *108*, 1040−1049.
(57) Hay, P.; Goodard, W. Theoretical results for the excited states of ozone. *Chem. Phys. Lett.* **1972**, *14*, 46−48.
(58) Theis, D.; Ivanic, J.; Windus, T. L.; Ruedenberg, K. The transition from the open minimum to the ring minimum on the ground state and on the lowest excited state of like symmetry in ozone: A configuration interaction study. *J. Chem. Phys.* **2016**, *144*, 104304.
(59) Tavan, P.; Schulten, K. Electronic excitations in finite and infinite polyenes. *Phys. Rev. B: Condens. Matter Mater. Phys.* **1987**, *36*, 4337−4358.
(60) Watts, J. D.; Gwaltney, S. R.; Bartlett, R. J. Coupled-cluster calculations of the excitation energies of ethylene, butadiene, and cyclopentadiene. *J. Chem. Phys.* **1996**, *105*, 6979−6988.
(61) Starcke, J. H.; Wormit, M.; Schirmer, J.; Dreuw, A. How much double excitation character do the lowest excited states of linear polyenes have? *Chem. Phys.* **2006**, *329*, 39−49.
(62) Li, X.; Paldus, J. Size dependence of the $X^1A_g \rightarrow 1^1B_u$ excitation energy in linear polyenes. *Int. J. Quantum Chem.* **1999**, *74*, 177−192.

DOI: 10.1021/acs.jpca.8b01554
J. Phys. Chem. A XXXX, XXX, XXX−XXX

(63) Nakayama, K.; Nakano, H.; Hirao, K. Theoretical study of the π-π^* excited states of linear polyenes: The energy gap between $1^1B_u^+$ and $2^1A_g^-$ states and their character. *Int. J. Quantum Chem.* **1998**, *66*, 157−175.
(64) Schreiber, M.; Silva-Junior, M. R.; Sauer, S. P. A.; Thiel, W. Benchmarks for electronically excited states: CASPT2, CC2, CCSD, and CC3. *J. Chem. Phys.* **2008**, *128*, 134110.
(65) Mazur, G.; Włodarczyk, R. Application of the dressed time-dependent density functional theory for the excited states of linear polyenes. *J. Comput. Chem.* **2009**, *30*, 811−817.
(66) Schmidt, M.; Tavan, P. Electronic excitations in long polyenes revisited. *J. Chem. Phys.* **2012**, *136*, 124309.
(67) Piecuch, P.; Hansen, J. A.; Ajala, A. O. Benchmarking the completely renormalised equation-of-motion coupled-cluster approaches for vertical excitation energies. *Mol. Phys.* **2015**, *113*, 3085−3127.
(68) Dunning, T. H. Gaussian basis sets for use in correlated molecular calculations. I. The atoms boron through neon and hydrogen. *J. Chem. Phys.* **1989**, *90*, 1007−1023.
(69) Kendall, R. A.; Dunning, T. H.; Harrison, R. J. Electron affinities of the first-row atoms revisited. Systematic basis sets and wave functions. *J. Chem. Phys.* **1992**, *96*, 6796−6806.
(70) Widmark, P.-O.; Malmqvist, P.-Å.; Roos, B. O. Density matrix averaged atomic natural orbital (ANO) basis sets for correlated molecular wave functions. *Theor. Chim. Acta* **1990**, *77*, 291−306.
(71) Daday, C.; Smart, S.; Booth, G. H.; Alavi, A.; Filippi, C. Full configuration interaction excitations of ethene and butadiene: Resolution of an ancient question. *J. Chem. Theory Comput.* **2012**, *8*, 4441−4451.
(72) Krylov, A. I.; Gill, P. M. W. Q-Chem: An engine for innovation. *Wiley Interdiscip. Rev. Comput. Mol. Sci.* **2013**, *3*, 317−326.
(73) Łoch, M. W.; Lodriguito, M. D.; Piecuch, P.; Gour, J. R. Two new classes of non-iterative coupled-cluster methods derived from the method of moments of coupled-cluster equations. *Mol. Phys.* **2006**, *104*, 2149−2172.
(74) Manohar, P. U.; Krylov, A. I. A noniterative perturbative triples correction for the spin-flipping and spin-conserving equation-of-motion coupled-cluster methods with single and double substitutions. *J. Chem. Phys.* **2008**, *129*, 194105.
(75) Schaefer, H. F. Methylene: A paradigm for computational quantum chemistry. *Science* **1986**, *231*, 1100−1107.
(76) Bauschlicher, C. W.; Taylor, P. R. A full CI treatment of the $^1A_1$-$^3B_1$ separation in methylene. *J. Chem. Phys.* **1986**, *85*, 6510−6512.
(77) Sherrill, C.; Van Huis, T. J.; Yamaguchi, Y.; Schaefer, H. F. Full configuration interaction benchmarks for the states of methylene. *J. Mol. Struct.: THEOCHEM* **1997**, *400*, 139−156.
(78) Zimmerman, P. M.; Toulouse, J.; Zhang, Z.; Musgrave, C. B.; Umrigar, C. J. Excited states of methylene from quantum Monte Carlo. *J. Chem. Phys.* **2009**, *131*, 124103.
(79) Slipchenko, L. V.; Krylov, A. I. Singlet-triplet gaps in diradicals by the spin-flip approach: A benchmark study. *J. Chem. Phys.* **2002**, *117*, 4694−4708.
(80) Shao, Y.; Head-Gordon, M.; Krylov, A. I. The spin-flip approach within time-dependent density functional theory: Theory and applications to diradicals. *J. Chem. Phys.* **2003**, *118*, 4807−4818.
(81) Chien, A. D.; Zimmerman, P. M. Iterative submatrix diagonalisation for large configuration interaction problems. *Mol. Phys.* **2018**, *116*, 107−117.
(82) Jensen, P.; Bunker, P. R. The potential surface and stretching frequencies of X^3B_1 methylene (CH_2) determined from experiment using the Morse oscillator-rigid bender internal dynamics Hamiltonian. *J. Chem. Phys.* **1988**, *89*, 1327−1332.
(83) Alijah, A.; Duxbury, G. Renner-Teller and spin-orbit interactions between the $^1A_1$, $^1B_1$, and $^3B_1$ states of CH_2. *Mol. Phys.* **1990**, *70*, 605−622.
(84) Davidson, E. R. The spatial extent of the V State of ethylene and its relation to dynamic correlation in the Cope rearrangement. *J. Phys. Chem.* **1996**, *100*, 6161−6166.
(85) Müller, T.; Dallos, M.; Lischka, H. The ethylene 1^1B_{1u} V state revisited. *J. Chem. Phys.* **1999**, *110*, 7176−7184.
(86) Angeli, C. An analysis of the dynamic σ polarization in the V state of ethene. *Int. J. Quantum Chem.* **2010**, *110*, 2436−2447.
(87) Mulliken, R. S. The excited states of ethylene. *J. Chem. Phys.* **1977**, *66*, 2448−2451.
(88) Moore, J. H.; Doering, J. P. Ion impact spectroscopy: Inelastic scattering of 150−500-eV H^+ and H_2^+ from N_2, CO, C_2H_2, and C_2H_4. *J. Chem. Phys.* **1970**, *52*, 1692−1699.
(89) Moore, J. H. Investigation of the low energy singlet-triplet and singlet-singlet transitions in ethylene derivatives by ion impact. *J. Phys. Chem.* **1972**, *76*, 1130−1133.
(90) Van Veen, E. Low-energy electron-impact spectroscopy on ethylene. *Chem. Phys. Lett.* **1976**, *41*, 540−543.
(91) Andersen, S. O.; Halberstadt, M. L.; Borgford-Parnell, N. Stratospheric ozone, global warming, and the principle of unintended consequences - An ongoing science and policy success story. *J. Air Waste Manage. Assoc.* **2013**, *63*, 607−647.
(92) Lee, T. J. On the energy separation between the open and cyclic forms of ozone. *Chem. Phys. Lett.* **1990**, *169*, 529−533.
(93) Qu, Z.-W.; Zhu, H.; Schinke, R. Infrared spectrum of cyclic ozone: A theoretical investigation. *J. Chem. Phys.* **2005**, *123*, 204324.
(94) Xantheas, S.; Elbert, S. T.; Ruedenberg, K. An intersection seam between the ground state of ozone and an excited state of like symmetry. *J. Chem. Phys.* **1990**, *93*, 7519−7521.
(95) Xantheas, S. S.; Atchity, G. J.; Elbert, S. T.; Ruedenberg, K. Potential energy surfaces of ozone. *J. Chem. Phys.* **1991**, *94*, 8054−8069.
(96) Atchity, G. J.; Ruedenberg, K. Global potential energy surfaces for the lowest two $^1A'$ states of ozone. *Theor. Chem. Acc.* **1997**, *96*, 176−194.
(97) Atchity, G. J.; Ruedenberg, K.; Nanayakkara, A. The intersection seam between the $1^1A'$ and $2^1A'$ states of ozone. *Theor. Chem. Acc.* **1997**, *96*, 195−204.
(98) An extrapolated value of −155.5578 was obtained by fitting the values in Table 6 of ref 12 to either a linear or a quadratic function of $1/M$, where M is the DMRG bond dimension.
(99) Komainda, A.; Lefrancois, D.; Dreuw, A.; Köppel, H. Theoretical study of the initial non-radiative $1B_u \rightarrow 2A_g$ transition in the fluorescence quenching of s-trans-butadiene: Electronic structure methods and quantum dynamics. *Chem. Phys.* **2017**, *482*, 27−38.
(100) Fuß, W.; Schmid, W.; Trushin, S. Ultrafast electronic relaxation of s-trans-butadiene. *Chem. Phys. Lett.* **2001**, *342*, 91−98.
(101) Watson, M. A.; Chan, G. K.-L. Excited states of butadiene to chemical accuracy: Reconciling theory and experiment. *J. Chem. Theory Comput.* **2012**, *8*, 4013−4018.
(102) Mosher, O. A.; Flicker, W. M.; Kuppermann, A. Electronic spectroscopy of s-trans 1,3-butadiene by electron impact. *J. Chem. Phys.* **1973**, *59*, 6502−6511.
(103) McDiarmid, R. On the ultraviolet spectrum of trans-1,3-butadiene. *J. Chem. Phys.* **1976**, *64*, 514−521.
(104) Doering, J. P.; McDiarmid, R. Electron impact study of the energy levels of tran-1,3-butadiene: II. Detailed analysis of valence and Rydberg transitions. *J. Chem. Phys.* **1980**, *73*, 3617−3624.
(105) Mosher, O. A.; Flicker, W. M.; Kuppermann, A. Triplet states in 1,3-butadiene. *Chem. Phys. Lett.* **1973**, *19*, 332−333.
(106) Hayden, C. C.; Chandler, D. W. Femtosecond time-delayed photoionization studies of ultrafast internal conversion in 1,3,5-hexatriene. *J. Phys. Chem.* **1995**, *99*, 7897−7903.
(107) Cyr, D. R.; Hayden, C. C. Femtosecond time-resolved photoionization and photoelectron spectroscopy studies of ultrafast internal conversion in 1,3,5-hexatriene. *J. Chem. Phys.* **1996**, *104*, 771−774.
(108) Ohta, K.; Naitoh, Y.; Tominaga, K.; Hirota, N.; Yoshihara, K. Femtosecond transient absorption studies of trans- and cis-1,3,5-hexatriene in solution. *J. Phys. Chem. A* **1998**, *102*, 35−44.
(109) Komainda, A.; Lyskov, I.; Marian, C. M.; Köppel, H. Ab initio benchmark study of nonadiabatic S_1-S_2 photodynamics of cis- and trans-hexatriene. *J. Phys. Chem. A* **2016**, *120*, 6541−6556.

DOI: 10.1021/acs.jpca.8b01554
J. Phys. Chem. A XXXX, XXX, XXX−XXX

(110) Fujii, T.; Kamata, A.; Shimizu, M.; Adachi, Y.; Maeda, S. Two-photon absorption study of 1,3,5-hexatriene by CARS and CSRS. *Chem. Phys. Lett.* **1985**, *115*, 369−372.
(111) Flicker, W. M.; Mosher, O. A.; Kuppermann, A. Low energy, variable angle electron-impact excitation of 1,3,5-hexatriene. *Chem. Phys. Lett.* **1977**, *45*, 492−497.

DOI: 10.1021/acs.jpca.8b01554
J. Phys. Chem. A XXXX, XXX, XXX−XXX